Supporting information for "Hydrophobic aggregation and collective absorption of dioxin into lipid membranes: insights from atomistic simulations"

Mosé Casalegno,[a], Guido Raos [a], and Guido Sello*[b]

[a] Dipartimento di Chimica, Materiali e Ingegneria Chimica "G. Natta", Politecnico di Milano, Via L. Mancinelli 7, 20131 Milano, Italy.
[b]Dipartimento di Chimica, Università degli Studi di Milano, Via C. Golgi 19, 20133 Milano, Italy. email: guido.sello@unimi.it.

Details of molecular dynamics simulations

In this work we performed both position-unrestrained (e.g. plain) and restrained MD simulations. All simulations were performed with the GROMACS-4.6 program suite[1]. Pressure and temperature are maintained at 1 atm and 325 K using the weak-coupling scheme[2]. The equations of motion were integrated using the leap-frog algorithm with a time step of 1 fs. Periodic boundary conditions were applied along all axes. TCDD, DPPC and water temperatures were coupled separately via velocity rescaling[3], with time constants of 0.1 ps. The pressure was controlled via semi-isotropic coupling to Berendsen barostats, with time constant of 1 ps and isothermal compressibilityof $4.6{\cdot}10^{-5}$ atm^{-1}. All non-bonded cut-off radii were set to 1.2 nm. Electrostatic interactions were treated via the Particle-Mesh Ewald method with a Fourier grid spacing of 0.12 nm. Hydrogen atoms were modeled explicitly, and no constraints were applied to bonds nor angles. As stated in the text, plain MD simulations were carried for systems with different number of TCDD molecules. The input file for all these systems was built starting from a pre-equilibrated bilayer containing 128 DPPC molecules in water[4]. The bilayer, oriented orthogonally to the z-axis, originally comprised 3655 water molecules. In order to give more room to the TCDD molecules, and prevent the bilayer to interact with its own top and bottom periodic images, the number of water molecules was doubled. Some empty space was left, in order to avoid bad contacts. Another program, written by our group, was used to insert the TCDD molecules in the aqueous phase. The insertion was accomplished removing a minimum number of water molecule surrounding the TCDD ones. The final number of water molecules, after the addition of TCDD was about 7000 in all systems. The resulting input was then equilibrated via a short (10-20 ns) NPT simulation in order to adjust the box size and correct the density. After this step, NPT production runs were performed in order to investigate the absorption and diffusion of TCDD into the membrane. Table S1 collects all the systems investigated in this work. For each system, we carried out up to 3 independent runs, made up by sequential simulations, each with a duration of 20-50 ns, depending on the availability of the CPU time. For some systems (N=1,5,10), the MD configurations with absorbed dioxin clusters were further used as starting input for MD simulations aimed at assessing the effects of sequential membrane loading. To this end, M dioxin molecules were added to the aqueous phase of equilibrated N-TCDD systems. The insertion of TCDD molecules was performed as explained above. For these systems, abbreviated as N+M-TCDD, we performed one run; other simulations are still in progress. It should be noted that some systems were more extensively investigated than others, depending on the time required to observe the dioxin cluster absorption. In the case of 10-TCDD, Run 2 and 3 were extended, in order to better study TCDD diffusion after absorption.

Beside plain MD simulations, we performed position-restrained calculations on the 1-TCDD system, in order to evaluate the free energy of absorption, the diffusion coefficients, and the dioxin permeability. These quantities were calculated via the force autocorrelation method[5]. In order to obtain more reliable results[6], the initial configurations in these simulations were taken from the unrestrained NPT runs described above. We performed five independent sets of calculations in which the z-distance between the TCDD and bilayer center-of-mass was progressively shortened from 4 to 0 nm, resulting in twenty-one equally spaced positions. For each position, a 20-ns NPT run was performed within each set. The overall simulation time

Table. S 1: Simulation times — in ns — taken by each run, for each of the systems considered. Each run comprised a variable number of sequential MD simulations, not reported for brevity.

System	Run 1	Run 2	Run 3
1-TCDD	20	103	77
2-TCDD	40	-	-
3-TCDD	143	55	74
5-TCDD	83	112	74
10-TCDD	53	686	630
1+1-TCDD	27	-	-
5+1-TCDD	20	-	-
10+10-TCDD	192	-	-

for each position sampled was therefore 100 ns. The forces acting on the dioxin molecule were saved every 10 MD steps, corresponding to 0.01 ps. For each set, both the average force acting on the TCDD molecule $\bar{F}(z) = \langle F(z,t) \rangle_t$, and the local diffusion coefficient, $D(z)$ were calculated. $D(z)$ was evaluated according to the force autocorrelation function method[5–7]:

$$D(z) = \frac{(RT)^2}{\int_0^\infty \langle \Delta F(z,t) \Delta F(z,t_0) \rangle \, dt}, \tag{S-1}$$

where $\Delta F(z,t) = F(z,t) - \bar{F}(z)$. We found the autocorrelation function to quickly approach zero. Therefore, the evaluation of the above integral was performed over a time interval of 10 ps. Following the procedure described by Allen et al.[8], Eq.(S-1) was evaluated starting from different time origins t_0, and the final result obtained as the average of ten individual estimates.
In order to improve the successive integral evaluation, both the average force and the local diffusion coefficients were interpolated via cubic splines[9]. 1000 sample points were adopted in both cases. Figure S1 shows the result of the interpolation for the average force obtained from set 1 simulations. Analogous results were obtained for the other sets. The free energy profile was obtained integrating the average force in the range from 4 to 0 nm:

$$\Delta G(z) = -\int_0^{+4} \langle F(z,t) \rangle_t \, dz \tag{S-2}$$

The value in the water phase (z = 4 nm) was taken as reference. For each set, the solute resistance profiles, $R(z)$, and the permeabilities were finally obtained according to the inhomogeneous solubility-diffusion model[5–7]. The permeability (P) was calculated integrating the solute resistance over the entire bilayer, from z = 4 to z = -4 nm:

$$P = 1 \,/ \int_{-4}^{+4} R(z) dz = 1 \,/ \int_{-4}^{+4} \frac{e^{\Delta G(z)/k_b T}}{D(z)} dz \tag{S-3}$$

Statistical convergence of free energy calculations

In this paragraph, we provide the results of numerical tests aimed at assessing the statistical convergence of equilibrium properties in our position-restrained simulations of the 1-TCDD system. In analogy with the approach suggested by Neale and co-workers[10], we have tested the convergence of the free energy as a function of the equilibration time (t_{eq}). To this end, the numerical values of the force associated with the simulation times shorter than t_{eq} were neglected in the calculation of the average force. Also in this case, the average forces along the z coordinate were obtained averaging over the five sets, and were subsequently interpolated via cubic splines. The equilibration time was progressively increased from 0 (all data) to 15

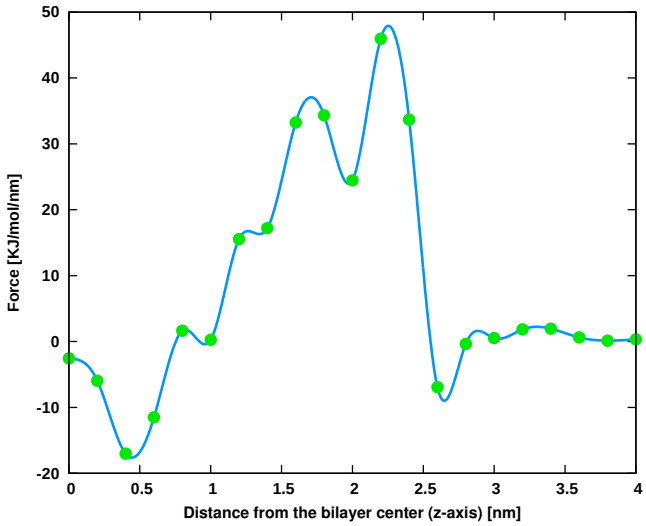

Fig. S 1: Original (green dots) and interpolated (blue line) average forces for set 1 simulations.

ns, with a 5 ns increment. The resulting free energy profiles are shown in Figure S2. The comparison of these profiles indicates that convergence was achieved for equilibration times equal or greater than 10 ns. As shown in the inset, discarding data beyond 10 ns increased the standard deviation around the free energy minimum. For this reason, the free energy profile corresponding to t_{eq}=10 ns was chosen as that most representative for the dioxin-membrane interaction in the 1-TCDD system (see Figure 2 in the text).

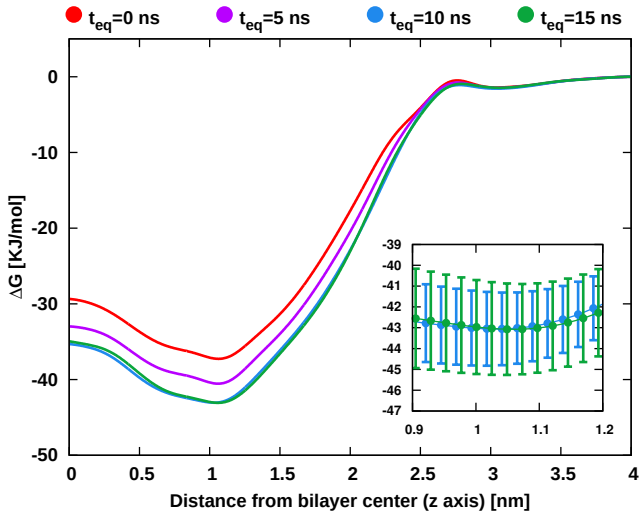

Fig. S 2: Free energy profiles obtained for different equilibration times. For better clarity the standard deviations have been omitted. The inset shows the profiles for t_{eq}=10 and t_{eq}=15 ns and the relative standard devations, around the free energy minimum. All profiles reported were obtained averaging over five sets of constrained simulations.

To further verify the convergence, we calculated the local diffusion coefficients increasing t_{eq}. The result is shown in figure S3. Also in this case, the profiles corresponding to t_{eq}=10 and t_{eq}=15 ns are closely similar.

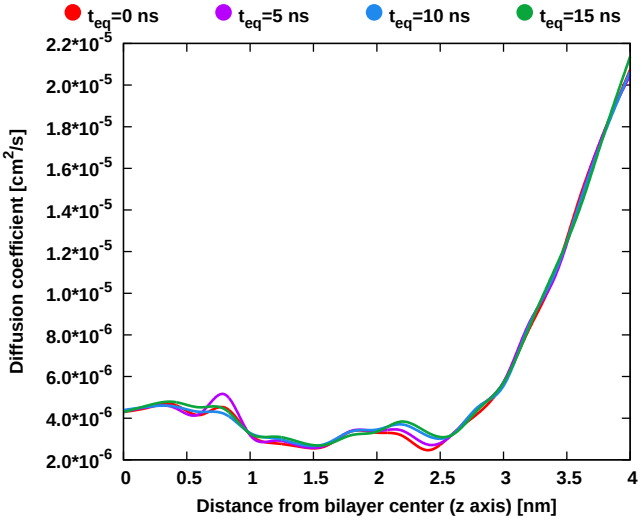

Fig. S 3: Local diffusion coefficient profiles obtained for different equilibration times. For better clarity the standard deviations have been omitted. All profiles reported were obtained averaging over five sets of constrained simulations.

Calculation of the structural and orientational parameters for 1-TCDD and 10-TCDD systems

In order to better characterize the TCDD absorption dynamics, and evaluate its effects on the DPCC membrane, we calculated geometrical and structural properties for the 1-TCDD and the 10-TCDD systems. These included: (a) the TCDD orientation with respect to the membrane surface, (b) the area-per-lipid, and (c) the membrane thickness. The TCDD orientation was taken as the tilt angle between the molecular plane and the vector normal to the bilayer surface. Thus an angle of 0° indicates that TCDD is orthogonal to the membrane. Figure S4 shows the result of this calculation for the 1-TCDD system. For comparison purposes, we also reported the distance from the bilayer center. During the absorption, the tilt angle of the TCDD molecule approaches small values, corresponding to an orientation perpendicular to the membrane surface. It is clear that this angle facilitates the penetration of the TCDD in the membrane. Once absorbed the TCDD changes its orientation, its angle now showing smaller fluctuations than those in bulk water. The situation is much more complex for the 10-TCDD system (not shown), where the dioxin molecules enter the membrane with different angles, due to dioxin-dioxin interactions. The molecular factors responsible for this outcome will be clarified in future works.

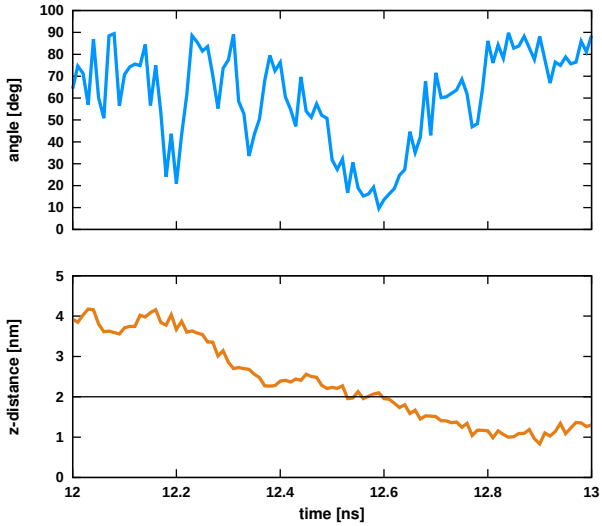

Fig. S 4: Dioxin tilt angle (top) and distance from bilayer center (bottom), versus the simulation time for the 1-TCDD system.

Figures S5 and S6 show the average area-per-lipid in 1- and 10-TCDD systems. In both cases, its value increases by about 0.01 nm^2 upon dioxin absoprtion. Surprisingly, the number of dioxin molecules had no significant effect on this increment. This is due to the fact the dioxin molecules are always absorbed sequentially rather than simultaneously.

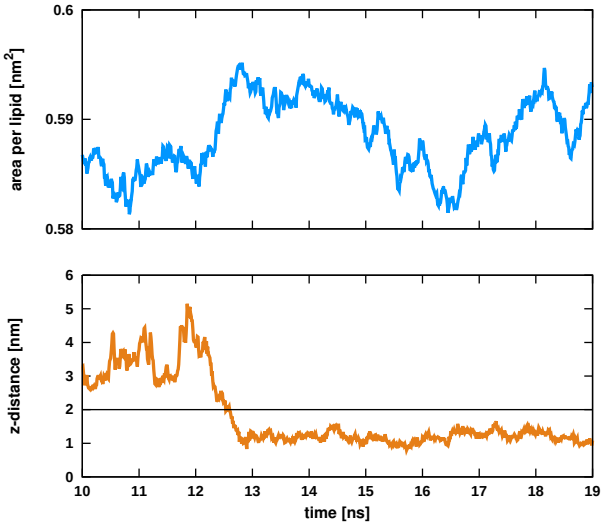

Fig. S 5: Area-per-lipid (top) and distance from the bilayer center (bottom), versus the simulation time for the 1-TCDD system.

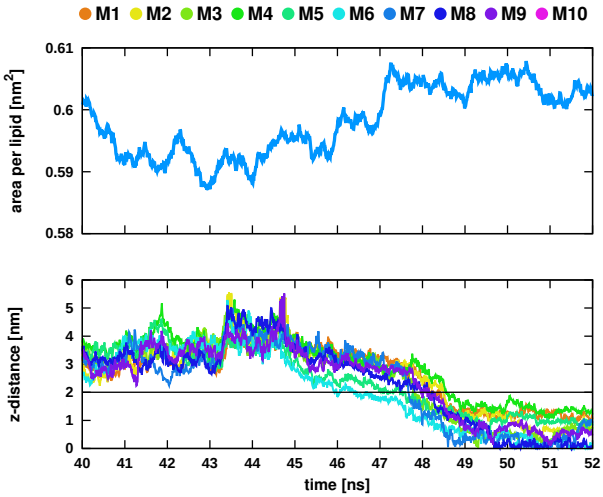

Fig. S 6: Area-per-lipid (top) and distance from the bilayer center (bottom), versus the simulation time for the 10-TCDD system.

The last two figures, Figure S7 and S8, show the change in the membrane thickness upon dioxin absorption for the two systems considered. The absorption of one TCDD molecule does not significantly affect the membrane thickness. For the 10-TCDD systems, the membrane thickness decreases during the absorption process. Its average value, however, is restored few nanoseconds after absorption.

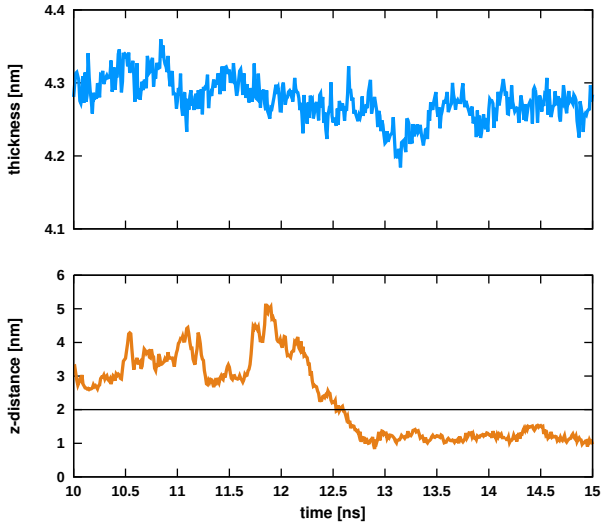

Fig. S 7: Membrane thickness (top) and distance the from bilayer center (bottom), versus the simulation time for the 1-TCDD system.

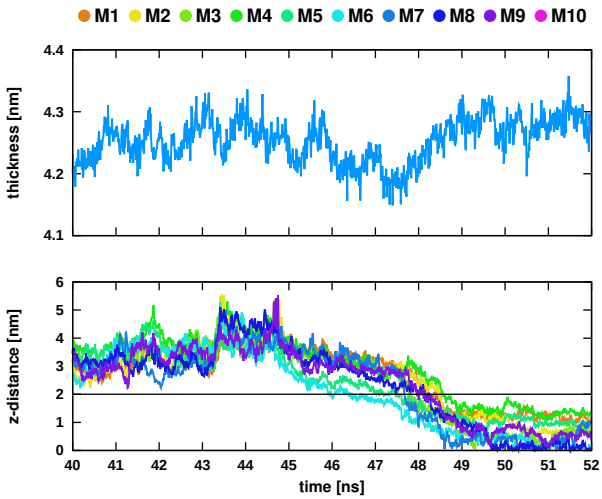

Fig. S 8: Membrane thickness (top) and distance the from bilayer center (bottom), versus the simulation time for the 10-TCDD system.

References

[1] D. van der Spoel, E. Lindahl, B. Hess, G. Groenhof, A. E. Mark, and H. J. C. Berendsen, *J. Comp. Chem.*, 2005 **26**, 1701; B. Hess, C. Kutzner, D. van der Spoel, and E. Lindahl, *J. Chem. Theory Comp.*, 2008, **4(3)**, 435.

[2] H. J. C. Berendsen, J. P. M. Postma, W. F. van Gunsteren, A. Di Nola, and J. R. Haak, *J. Chem. Phys.*, 1984, **81**, 3684.

[3] G. Bussi, D. Donadio, and M. Parrinello, *J. Chem. Phys.*, 2007, **126**, 014101.

[4] J. P. Ulmschneider and M. B. Ulmschneider, *J. Chem. Theory Comput.*, 2009, **5**, 1803.

[5] S. J. Marrink and H. J. C. Berendsen, *J. Phys. Chem.*, 1994, **98**, 4155.

[6] M. Paloncýová, K. Berka, and M. Otyepka, *J. Chem. Theory Comput.*, 2012, **8(4)**, 1200.

[7] M. Orsi, W. E. Sanderson, and J. W. Essex, *J. Phys. Chem. B*, 2009, **113**, 12019.

[8] M. P. Allen and D. J. Tildesley, in Computer Simulation of Liquids, Clarendon Press, Oxford, UK, 1989, ch. 6, pp. 185-188.

[9] T. Williams and C. Kelley, Gnuplot 4.5: an interactive plotting program. URL http://gnuplot.info. (Last accessed: 2014 November 17).

[10] C. Neale, W. F. D. Bennett, D. P. Tieleman, and R. Pomès *J. Chem. Theory Comput.*, 2011, **7(12)**, 4175; J. P. M. Jambeck and A. P. Lyubartsev, *J. Phys. Chem. Lett.*, 2013, **4**, 1781.